

Numerical Study on Fabrication Tolerance of Half-Ridge InP Polarization Converters

Masaru ZAITSU^{†a)}, Student Member, Takuo TANEMURA[†], Member, and Yoshiaki NAKANO[†], Fellow

SUMMARY Integrated InP polarization converters based on half-ridge structure are studied numerically. We demonstrate that the fabrication tolerance of the half-ridge structure can be extended significantly by introducing a slope at the ridge side and optimizing the thickness of the residual InGaAsP layer. High polarization conversion over 90% is achieved with the broad range of the waveguide width from 705 to 915 nm, corresponding to a factor-of-two or larger improvement in the fabrication tolerance compared with that of the conventional polarization converters. Finally we present a simple fabrication procedure of this newly proposed structure, where the thickness of the residual InGaAsP layer is controlled precisely by using a thin etch-stop layer.

key words: Polarization converters, fabrication tolerances, monolithic integration, polarization-multiplexing, photonic integrated circuits

1. Introduction

The number of optical components and the complexity in the optical communication systems have been increasing for adapting to the expansion of the channel capacity in the wavelength division multiplexing (WDM) and more advanced coherent modulation formats. Polarization division multiplexing (PDM) has been recently applied in the optical transmission links as a powerful technique to double the spectral efficiency. Meanwhile, photonic integrated circuits (PICs) have been demonstrated to reduce the cost and size of such highly complicated optical transceivers. There has been a growing interest in realizing compact and low-cost PDM optical transceivers by using the PICs [1]–[4]. In order to manipulate the dual polarization states inside the PICs and realize fully integrated PDM-PICs, integrated polarization converters (PCs) are essential.

Various types of PCs have been demonstrated to date; those based on periodic loaded waveguides [5], micro-bended waveguides [6], adiabatic waveguides [7]–[10], and asymmetric waveguides [11]–[19]. The asymmetric PCs are suitable for monolithic integration with InP photonic devices as well as their short operating length and relatively small sensitivity against the deviation of the wavelength and the temperature. However, integration of the InP PCs with laser diodes (LDs) and other active components has been challenging. First, most asymmetric PCs are fabricated on

rib waveguide, while other components in InP-PICs usually have ridge structures. Such structural mismatch often leads to large coupling losses and requires relatively complicated fabrication procedures which may not suit the generic fabrication technologies [20]. Another important issue is the strict fabrication tolerances of these types of PCs, where both the waveguide width and lithographic alignment have to be controlled within typically 100-nm accuracy. In this respect, a simple PC with a ridge-like waveguide structure having large fabrication tolerances is highly desired.

We have recently proposed and experimentally demonstrated a half-ridge InP/InGaAsP PC, which particularly suits the integration with LDs because of its ridge-like structure and a simple self-aligned fabrication process [21], [22]. More than 96% polarization conversion has been experimentally obtained with the PC length of 150 μm and the wide wavelength range covering the entire C-band.

In this paper, we numerically study the efficiency and the fabrication tolerances of this InP half-ridge PC. We demonstrate that a residual InGaAsP layer with a slope at the ridge side plays a crucial role in extending the tolerance against the deviation of the waveguide width. A factor-of-two improvement in fabrication tolerance is obtained with the optimized design. In addition, we propose a novel design of the layerstack with a thin etch-stop layer for controlling the thickness of the residual InGaAsP layer precisely. We then propose a simple fabrication procedure for the newly proposed half-ridge PC with an improved design.

2. Device structure and numerical model

Figure 1 shows the structure of the InP half-ridge PC, having an asymmetric cross section: One side of the waveguide has a shallow ridge structure with a residual InGaAsP core layer and the other has a deeply-etched high-mesa structure.

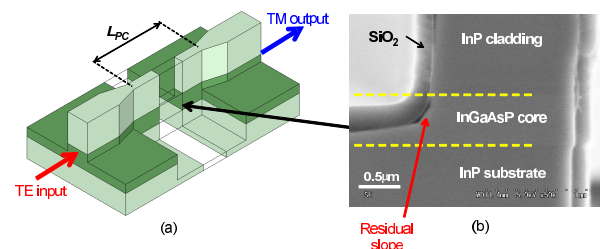


Fig. 1 (a) Schematic of the integrated half-ridge PC, (b) Cross-section image of the fabricated PC [22].

Manuscript received November 14, 2013.

Manuscript revised January 17, 2014.

[†]The authors are with the Department of Electrical Engineering and Information Systems (EEIS), Graduate School of Engineering, The University of Tokyo, Hongo, Bunkyo-ku, Tokyo 113-8656, Japan.

a) E-mail: zaitso@hotaka.t.u-tokyo.ac.jp

DOI: 10.1587/transele.E97.C.731

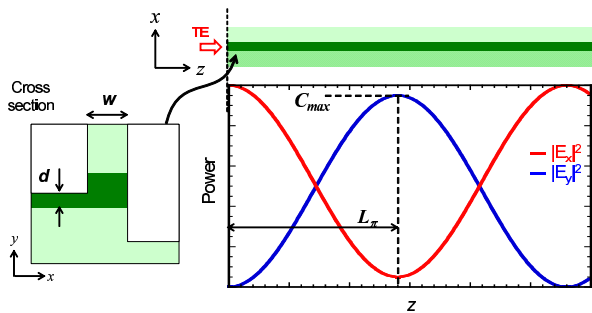


Fig. 2 Polarization conversion inside asymmetric waveguides.

By optimizing the waveguide width w and the residual core thickness d (see Fig. 2), this asymmetric waveguide operates as a birefringent medium with the principal axis rotated by $\pm 45^\circ$. In such a case, as shown in Fig. 2, a horizontally polarized, transverse electric (TE) mode input light excites the two eigenmodes in the PC with an equal magnitude, which would recombine into a vertically polarized, transverse magnetic (TM) mode after propagating the half-beat length [$L_\pi = \pi / (\beta_1 - \beta_2)$, where β_m is the propagation constant of mode m in the half-ridge PC].

The eigenmodes in a given cross-sectional structure of the PC are calculated by using a full-vector finite difference method [23]. As a measure of the angle of equivalent principal axes of the eigenmodes, we define the rotation parameter R by

$$R \equiv \frac{\iint |H_x|^2 dx dy}{\iint |H_y|^2 dx dy} \quad (1)$$

where H_x and H_y are the x - and y -components of the magnetic fields of the eigenmode, respectively. This parameter approximately expresses a rotation angle θ of the principal axes of the eigenmodes in waveguides as

$$R \approx \frac{|H_x|^2}{|H_y|^2} = 1 / \tan^2 \theta. \quad (2)$$

The maximum conversion ratio C_{max} is approximately expressed by R as

$$C_{max} = \sin^2 2\theta \approx \frac{4R}{(1+R)^2}. \quad (3)$$

A net TE-to-TM conversion ratio C is expressed by using C_{max} and L_π as

$$C = C_{max} \cdot \frac{1}{2} \left\{ 1 - \cos \left(\frac{\pi}{L_\pi} L_{PC} \right) \right\} \quad (4)$$

where L_{PC} is the length of the PC section. The TE-to-TM conversion ratio follows Eq. 4, a sinusoidal function of L_{PC} as shown in Fig. 2.

In our previous demonstration [22], the fabricated device had a residual slope at the ridge side of the InGaAsP core as shown in Fig. 1(b), which was due to a slight anisotropic etching during the Cl_2/Ar dry-etching process. In order to allow direct comparison with the actual devices,

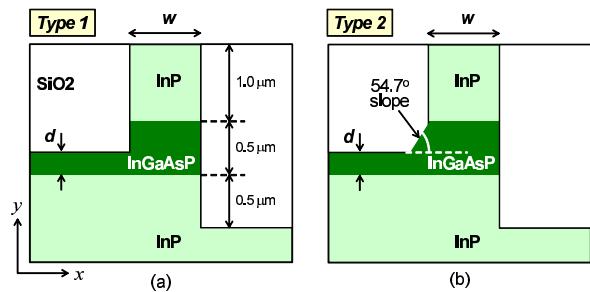


Fig. 3 Cross-section structure of the half-ridge PC: (a) Type 1 has a rectangular ridge side. (b) Type 2 has a 54.7° residual slope on the InGaAsP core which reflects the structure of the actual device shown in Fig. 1.

we assume two types of half-ridge PCs in our calculation. They have different cross-sectional structures as shown in Fig. 3. Type 1 has a rectangular etching profile at the ridge side as designed initially [21]. On the other hand, Type 2 has a 54.7° slope corresponding to (111) crystal plane of the InGaAsP, which reflects the actual fabricated device [22]. The eigenmodes in each structure are calculated for various values of the width of the PC w and the residual InGaAsP thickness d at the ridge side. The thicknesses of the InP top cladding, the InGaAsP entire core, and the overetched depth of the InP bottom cladding are fixed to be $1.0 \mu\text{m}$, $0.50 \mu\text{m}$, and $0.50 \mu\text{m}$, respectively. The refractive indices of InP, InGaAsP, and background (SiO_2) are set to 3.17, 3.40, and 1.45, respectively. The wavelength is set to $1.55 \mu\text{m}$ during the simulation.

3. Numerical results

Figures 4 and 5 show the calculated C_{max} and L_π as a function of w and d for Type 1 and Type 2, respectively. In both types, a conversion ratio of more than 99% is obtained by selecting w and d appropriately. We see from the figures that both C_{max} and L_π become less sensitive to w as we increase d from 0 to $0.30 \mu\text{m}$. This implies that the residual InGaAsP layer at the ridge side has a crucial role of extending the tolerance against the fabrication error in w . We also see that the fabrication tolerances in both w and d are larger for Type 2 compared with Type 1; the residual slope at the ridge side contributes to the increase in the tolerances. In the case of asymmetric PCs, triangular shape is the most ideal cross sectional structure to obtain efficient TE-to-TM conversion with short length [24]. The residual slope on the InGaAsP makes the light-confinement structure closer to the triangular shape, and therefore the tolerances in Type 2 is enlarged compared with Type 1.

The fabrication tolerance of an actual PC with a fixed length L_{PC} can be calculated by inserting the results plotted in Fig. 4 or 5 into Eq. 4. First, we select w and d at which C_{max} approaches 100%, and set $L_{PC} = L_\pi$. Under this fixed length of L_{PC} , the allowed range of w and d can be obtained from Eq. 4 and Fig. 4 or 5.

Figure 6 shows the calculated net conversion C for Type 1 and Type 2 as a function of w at $d = 0.30 \mu\text{m}$. L_{PC} is fixed to $200 \mu\text{m}$ for Type 1 and $100 \mu\text{m}$ for Type 2, which are

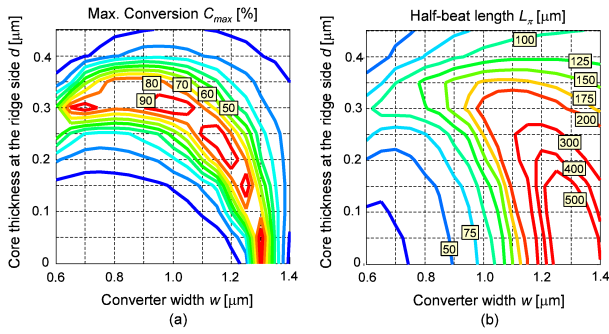


Fig. 4 Calculation result for Type 1 structure: (a) Maximum conversion ratio C_{max} , (b) Half-beat length L_{π} as a function of w and d .

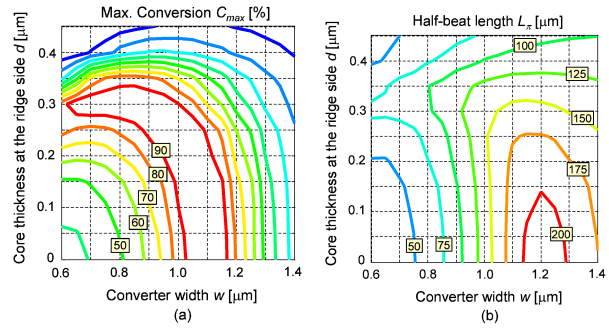


Fig. 5 Calculation result for Type 2 structure: (a) Maximum conversion ratio C_{max} , (b) Half-beat length L_{π} as a function of w and d .

the optimized length to maximize the fabrication tolerance of w . From Fig. 6, we see that a higher net conversion than 90% is obtained with $w = 810 \pm 105$ nm for Type 2, while $w = 1000 \pm 50$ nm for Type 1. We thus achieve factor-of-two improvement in the fabrication tolerance by using Type 2 over Type 1. Moreover, the half-beat length of Type 2 is also reduced to half than that of Type 1. We should note that this value of fabrication tolerance is larger than other types of asymmetric InP PCs [12], [15], and is readily achieved by the current fabrication technology.

4. Proposal of a width-tolerant PC using a novel layer-stack

Figure 7 shows the proposed procedure to fabricate Type 2 PC. As we have demonstrated in the previous section, the precise control of the thickness of the residual InGaAsP layer d is crucial in achieving a high fabrication tolerance in w . To this end, we propose to introduce a few-nm-thick InP etch-stop layer at the middle of the InGaAsP core. After forming a ridge waveguide along $[01\bar{1}]$ direction by dry etching (a), we selectively wet-etch InGaAsP layer until the InP etch-stop layer, so that a precisely defined slope corresponding to the (111) plane is formed. Similar to the half-ridge fabrication procedure [22], SiO₂ is deposited from an angle, covering only one side of the ridge waveguide (c). Finally, the Type 2 structure is obtained after the second dry-etching (d).

The etching depth of the InGaAsP can be precisely controlled with a nanometer-scale precision by using the

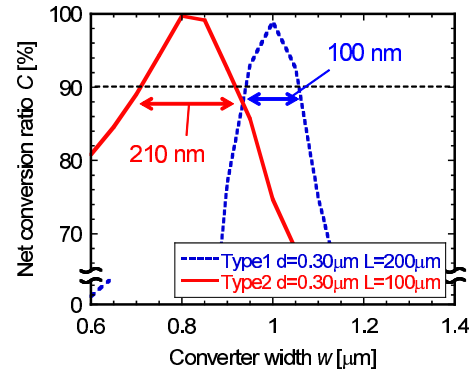


Fig. 6 Calculated net conversion ratio C as a function of converter width w , using Type 1 PC, $L_{PC} = 200 \mu\text{m}$ (dashed line), and Type 2 PC, $L_{PC} = 100 \mu\text{m}$ (solid line).

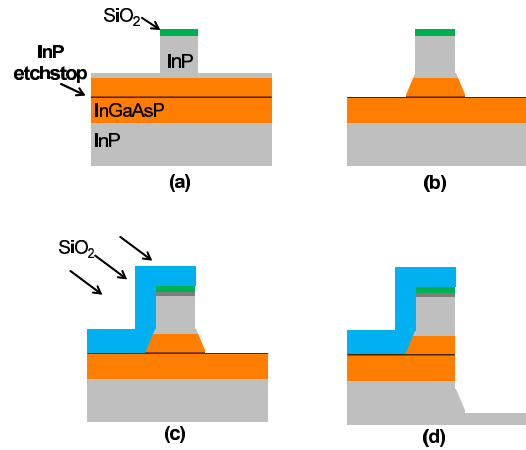


Fig. 7 Fabrication procedure of Type 2 PC using an InP etch-stop layer at the middle of the InGaAsP core.

InP etch-stop layer, owing to the excellent selectivity of the chemical etching process such as $\text{H}_2\text{SO}_4 + \text{H}_2\text{O}_2 + \text{H}_2\text{O}$ system [25]. Consequently, we can precisely tune the value of d in Type 2 PC. Although there would be a slight undercut during the InGaAsP wet etching, this effect should be negligible or easily calibrated because the total etching depth in this case is $0.20 \mu\text{m}$ and the etching rate of (111) plane is much slower than (100) plane.

5. Conclusion

We have presented numerical analyses on the integrated InP/InGaAsP PCs based on the half-ridge structure. From the analyses of both the original design (Type 1) and the actual fabricated structure (Type 2), we have revealed that the residual InGaAsP layer, as well as the slope at the ridge side plays an important role in extending the tolerances against fabrication errors. As an example case, we have demonstrated a high polarization conversion over 90% with a broad range of the waveguide width from 705 to 915 nm. Finally, we proposed a simple fabrication procedure of this new type of PC, where a thin etch-stop layer was introduced to control the thickness of the residual InGaAsP layer precisely. With the inherent compatibility with other active InP

components and simple self-aligned fabrication process, the demonstrated half-ridge PCs should pave the way to realize large-scale fully integrated PDM-PICs.

Acknowledgments

This work was supported by the Strategic Information and Communications R&D Promotion Programme (SCOPE), the Ministry of Internal Affairs and Communications of Japan, and Research Fellowships for Young Scientists, Japan Society for the Promotion of Science (JSPS).

References

- [1] M. Kato, P. Evans, S. Corzine, J. Gheorma, M. Fisher, M. Raburn, A. Dentai, R. Salvatore, I. Lyubomirsky, A. Nilsson, J. Rahn, R. Nagarajan, C. Tsai, B. Behnia, J. Stewart, D. Christini, M. Missey, A. Spannagel, D. Lambert, S. Agashe, P. Liu, D. Pavinski, M. Reffle, R. Schneider, M. Ziari, C. Joyner, F. Kish, and D. Welch, "Transmitter PIC for 10-channel \times 40 Gb/s per channel polarization-multiplexed RZ-DQPSK modulation," in *proc. Optical Fiber Communication Conference (OFC2009)*, paper OThN2, San Diego, CA, USA, Mar. 2009.
- [2] H. Yamazaki, T. Yamada, T. Goh, and A. Kaneko, "PDM-QPSK modulator with a hybrid configuration of silica PLCs and LiNbO₃ phase modulators," *J. Lightw. Technol.*, vol. 29, no. 5, pp. 721–727, Mar. 2011.
- [3] R. Nagarajan, J. Rahn, M. Kato, J. Pleumeekers, D. Lambert, V. Lal, H. S. Tsai, A. Nilsson, A. Dentai, M. Kuntz, R. Malendevich, J. Tang, J. Zhang, F. Butrie, M. Raburn, B. Little, W. Chen, G. Goldfarb, V. Dominic, B. Taylor, M. Reffle, F. Kish, and D. Welch, "10 channel, 45.6 Gb/s per channel, polarization-multiplexed DQPSK, InP receiver photonic integrated circuit," *J. Lightw. Technol.*, vol. 29, no. 4, pp. 386–395, Feb. 2011.
- [4] C.R. Doerr, N.K. Fontaine, and L.L. Buhl, "PDM-DQPSK silicon receiver with integrated monitor and minimum number of controls," *Photon. Technol. Lett.*, vol. 24, no. 8, pp. 697–699, Apr. 2012.
- [5] Y. Shani, R. Alferness, T. L. Koch, U. Koren, M. Oron, B. I. Miller, and M. G. Young, "Polarization rotation in asymmetric periodic loaded rib waveguides," *Appl. Phys. Lett.*, vol. 59, no. 11, pp. 1278–1280, Sept. 1991.
- [6] C. van Dam, L. H. Spiekman, F. P. G. M. van Ham, F. H. Groen, J. J. G. M. van der Tol, I. Moerman, W. W. Pascher, M. Hamacher, H. Heidrich, C. M. Weinert, and M.K. Smit, "Novel compact polarization converters based on ultra short bends," *IEEE Photon. Technol. Lett.*, vol. 8, no. 10, pp. 1346–1348, Oct. 1996.
- [7] M. R. Watts and H. A. Haus, "Integrated mode-evolution-based polarization rotators," *Opt. Lett.*, vol. 30, no. 2, pp. 138–140, Jan. 2005.
- [8] T. Barwicz, M. R. Watts, M. A. Popović, P. T. Rakich, L. Socci, F. X. Kärtner, E. P. Ippen, and H. I. Smith, "Polarization-transparent microphotonic devices in the strong confinement limit," *Nat. Photonics*, vol. 1, pp. 57–60, Jan. 2006.
- [9] H. Fukuda, K. Yamada, T. Tsuchizawa, T. Watanabe, H. Shinojima, and S. Itabashi, "Polarization rotator based on silicon wire waveguides," *Opt. Express*, vol. 16, no. 4, pp. 2628–2635, Feb. 2008.
- [10] J. Zhang, T. Y. Liow, M. Yu, G. Q. Lo, and D.L. Kwong, "Silicon waveguide based TE mode converter," *Opt. Express*, vol. 18, no. 24, pp. 25264–25270, Nov. 2010.
- [11] J. Z. Huang, R. Scarmozzino, G. Nagy, M. J. Steel, and R. M. Osgood, Jr., "Realization of a compact and single-mode optical passive polarization converter," *IEEE Photon. Technol. Lett.*, vol. 12, no. 3, pp. 317–319, Mar. 2000.
- [12] H. El-Refaei, D. Yevick, and T. Jones, "Slanted-rib waveguide InGaAsP-InP polarization converters," *J. Lightw. Technol.*, vol. 22, no. 5, pp. 1352–1357, May 2004.
- [13] M. V. Kotlyar, L. Bolla, M. Midrio, L. O'Faolain, and T. F. Krauss, "Compact polarization converter in InP-based material," *Opt. Express*, vol. 13, no. 13, pp. 5040–5045, June 2005.
- [14] D. M. Beggs, M. Midrio, and T. F. Krauss, "Compact polarization rotators for integrated polarization diversity in InP-based waveguides," *Opt. Lett.*, vol. 32, no. 15, pp. 2176–2178, Aug. 2007.
- [15] L. M. Augustin, J. J. G. M. van der Tol, E. J. Geluk, and M. K. Smit, "Short polarization converter optimized for active-passive integration in InGaAsP-InP," *IEEE Photon. Technol. Lett.*, vol. 19, no. 20, pp. 1673–1675, Oct. 2007.
- [16] S.-H. Kim, R. Takei, Y. Shoji, and T. Mizumoto, "Single-trench waveguide TE-TM mode converter," *Opt. Express*, vol. 17, no. 14, pp. 11267–11273, Jul. 2009.
- [17] C. Alonso-Ramos, S. Romero-García, A. Ortega-Moñux, I. Molina-Fernández, R. Zhang, H. G. Bach, and M. Schell, "Polarization rotator for InP rib waveguide," *Opt. Lett.*, vol. 37, no. 3, pp. 335–337, Feb. 2012.
- [18] M. Aamer, A. Gutierrez, A. Brimont, D. Vermeulen, G. Roelkens, J. M. Fedeli, A. Hakansson, and P. Sanchis, "CMOS compatible silicon-on-insulator polarization rotator based on symmetry breaking of the waveguide cross section," *Photon. Technol. Lett.*, vol. 24, no. 22, pp. 2031–2034, Nov. 2012.
- [19] D. O. Dzibrou, J. J. G. M. van der Tol, and M. K. Smit, "Improved fabrication process of low-loss and efficient polarization converters in InP-based photonic integrated circuits," *Opt. Lett.*, vol. 38, no. 7, pp. 1061–1063, Apr. 2013.
- [20] M. Smit, J. van der Tol, and M. Hill, "Moore's law in photonics," *Laser & Photon. Rev.*, vol. 6, no. 1, pp. 1–13, Jan. 2012.
- [21] T. Tanemura, T. Amemiya, K. Takeda, A. Higo, and Y. Nakano, "Simple and compact InP polarization converter for polarization-multiplexed photonic integrated circuits," *Proc. 22nd Annual Meeting of IEEE Lasers and Electro-Optics Society (LEOS2009)*, paper WF4, Belek-Antalya, Turkey, Oct. 2009.
- [22] M. Zaitso, T. Tanemura, A. Higo, and Y. Nakano, "Experimental demonstration of self-aligned InP/InGaAsP polarization converter for polarization multiplexed photonic integrated circuits," *Opt. Express*, vol. 21, no. 6, pp. 6910–6918, Mar. 2013.
- [23] P. Lüsse, P. Stuwe, J. Schüle, and H. G. Unger, "Analysis of vectorial mode fields in optical waveguides by a new finite difference method," *J. Lightw. Technol.*, vol. 12, no. 3, pp. 487–494, Mar. 1994.
- [24] J. Yamauchi, M. Yamanoue, and H. Nakano, "A short polarization converter using a triangular waveguide," *J. Lightw. Technol.*, vol. 26, no. 12, pp. 1708–1714, June 2008.
- [25] F. Fiedler, A. Schlachetzki, and G. Klein, "Material-selective etching of Inp and an InGaAsP alloy," *J. Mater. Sci.*, vol. 17, no. 10, pp. 2911–2918, Oct. 1982.



Masaru Zaitzu received the B.E. and M.S. degrees in Electronic Engineering from the University of Tokyo, Tokyo, Japan, in 2009 and 2011, respectively. He is currently a Ph.D. student in Dept. Electronic Engineering and Information Systems (EIS), School of Engineering, the University of Tokyo. He is a student member of IEEE photonics society, the Institute of Electronics, Information and Communication Engineers (IEICE) of Japan, and Japan Society of Applied Physics (JSAP). His research interests

includes semiconductor photonic integrated circuits and polarization handling devices.



Takuo Tanemura received the B.E., M.S., and Ph.D. degrees in Electronic Engineering, all from the University of Tokyo, Japan, in 2001, 2003, and 2006, respectively. In 2006, he joined the Department of Electronic Engineering, the University of Tokyo and moved to the Research Center for Advanced Science and Technology, the University of Tokyo in 2007 as a Lecturer. In April 2012, he moved back to the Department of Electronic Engineering, the University of Tokyo, and became Associate Professor.

From March 2010 to February 2012, he was a Visiting Scholar at Ginzton Laboratory, Stanford University. His research interest includes semiconductor photonic integrated circuits, nanophotonic and nanometallic devices, photonic switching networks, and optical interconnection. Dr. Tanemura is a member of IEEE and the Institute of Electronics, Information and Communication Engineers (IEICE) of Japan. He was the recipient of the 2005 IEEE Photonics Society Graduate Student Fellowships and Ericsson Young Scientist Award 2006.



Yoshiaki Nakano is the director and professor at the Research Center for Advanced Science and Technology, the University of Tokyo. He is also with the Department of Electronic Engineering, School of Engineering, the University of Tokyo. He received the B.E., M.S., and Ph.D. degrees in electronic engineering, all from the University of Tokyo, Japan, in 1982, 1984, and 1987, respectively. In 1984, he spent a year at the University of California, Berkeley, as an exchange student. In 1987, he joined the

Department of Electronic Engineering, the University of Tokyo, became Associate Professor in 1992, Professor in 2000, and the Department Head in 2001. He moved to the Research Center for Advanced Science and Technology, the University of Tokyo, in 2002, and became the director of the center in 2010. His research interests have been physics and fabrication technologies of semiconductor distributed feedback lasers, semiconductor optical modulators/switches, monolithically-integrated photonic circuits, and high-efficiency heterostructure solar cells. In 1992, he was a visiting Associate Professor at the University of California, Santa Barbara. Dr. Nakano was an elected member of the Board of Governors of IEEE LEOS, a member of the Board of Directors of the Japan Society of Applied Physics (JSAP), the Editor-in-Chief of Applied Physics Express (APEX) and Japanese Journal of Applied Physics (JJAP), and a member of the Board of Directors of the Japan Institute of Electronics Packaging (JIEP). He is currently the chairman of the Optoelectronics Technology Trend Research Committee of the Optoelectronics Industry and Technology Development Association (OITDA), and the chairman of the Optical Interconnect Standardization Committee of Japan Electronics Packaging

and Circuits Association (JPCA). He is also Fellow of the Institute of Electronics, Information, and Communication Engineers (IEICE), Fellow of JSAP, and a member of IEEE EDS and OSA. He served as the project leader of Japanese National Project on "Photonic Networking Technology" organized by the Ministry of Economy, Trading, and Industry (METI), and as the project leader of SORST Program on "Non-reciprocal Semiconductor Digital Photonic Integrated Circuits and their Applications to Photonic Networking" sponsored by Japan Science and Technology Corporation. He is currently the project leader of METI National R&D Project on "Post-Silicon Solar Cells for Ultra-High Efficiencies." He is the recipient of the 1987 Shinohara Memorial Prize from the IEICE, the 1991 Optics Paper Award from the JSAP, the 1997 Marubun Science Prize, the 2007 Ichimura Prize, the 2007 IEICE Electronics Society Award, and the 2007 Sakurai Medal from the OITDA. He was presented the Prime Minister Award in Collaborative Research between Academia and Industry in 2007. He authored and coauthored over 250 refereed journal publications and over 450 international conference papers, and holds 40 patents.